Supplementary Information

The Control of the Adsorption of Doxorubicin on Gold Surfaces Tracked by Surface-Enhanced Raman Scattering Spectroscopy

Pedro Victor A. Pessanha[a] *and Antonio Carlos Sant'Ana*[*,a]

[a]*Laboratório de Nanoestruturas Plasmônicas, Instituto de Ciências Exatas, Universidade Federal de Juiz de Fora, Rua José Lourenço Kelmer, s/n, Martelos, 36036-900 Juiz de Fora-MG, Brazil*

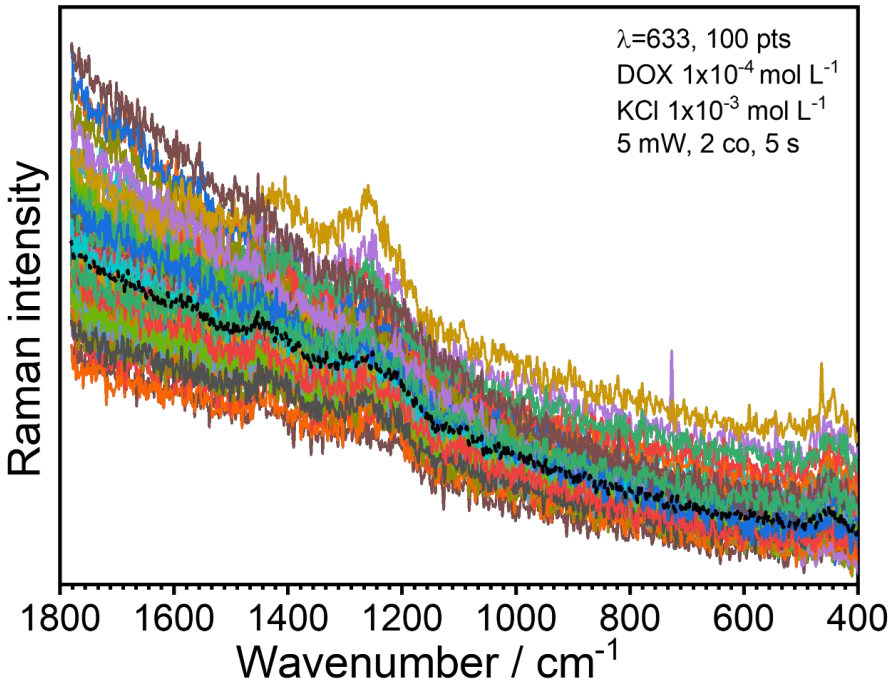

Figure S1. SERRS spectra of 1×10^{-4} mol L^{-1} doxorubicin adsorbed on AuNPs dry film, modified before drying with KCl, with final concentration of 1×10^{-3} mol L^{-1}. 100 points obtained with $\lambda_0 = 632.8$ nm.

*e-mail: antonio.sant@ufjf.br

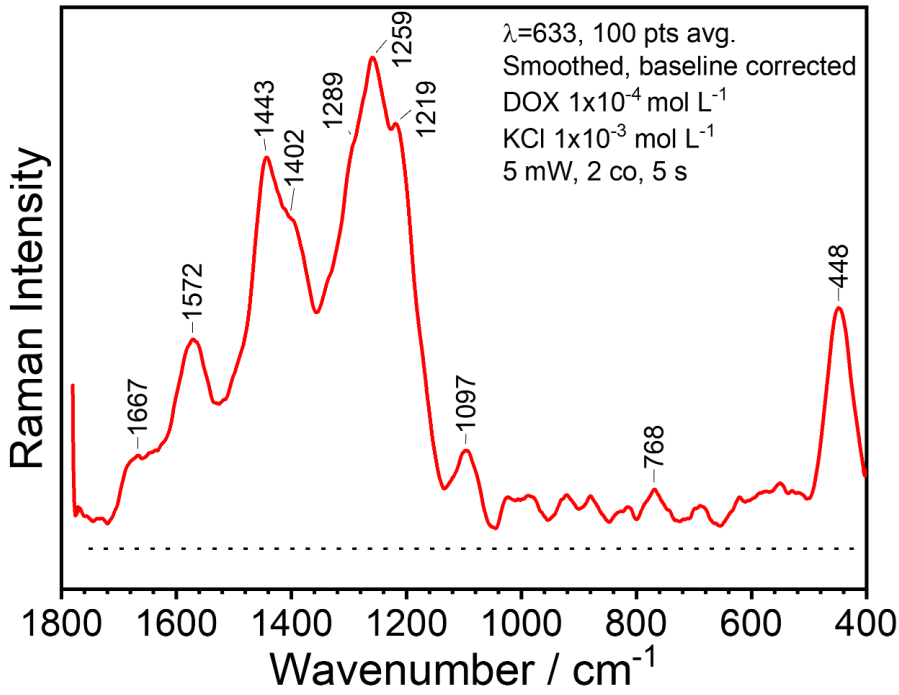

Figure S2. Average SERRS spectra of 1×10^{-4} mol L^{-1} DOX from 100 points, after baseline corrected and smoothed, recorded on AuNP dry film, modified before drying with KCl, with final concentration of 1×10^{-3} mol L^{-1}, obtained with $\lambda_0 = 632.8$ nm.

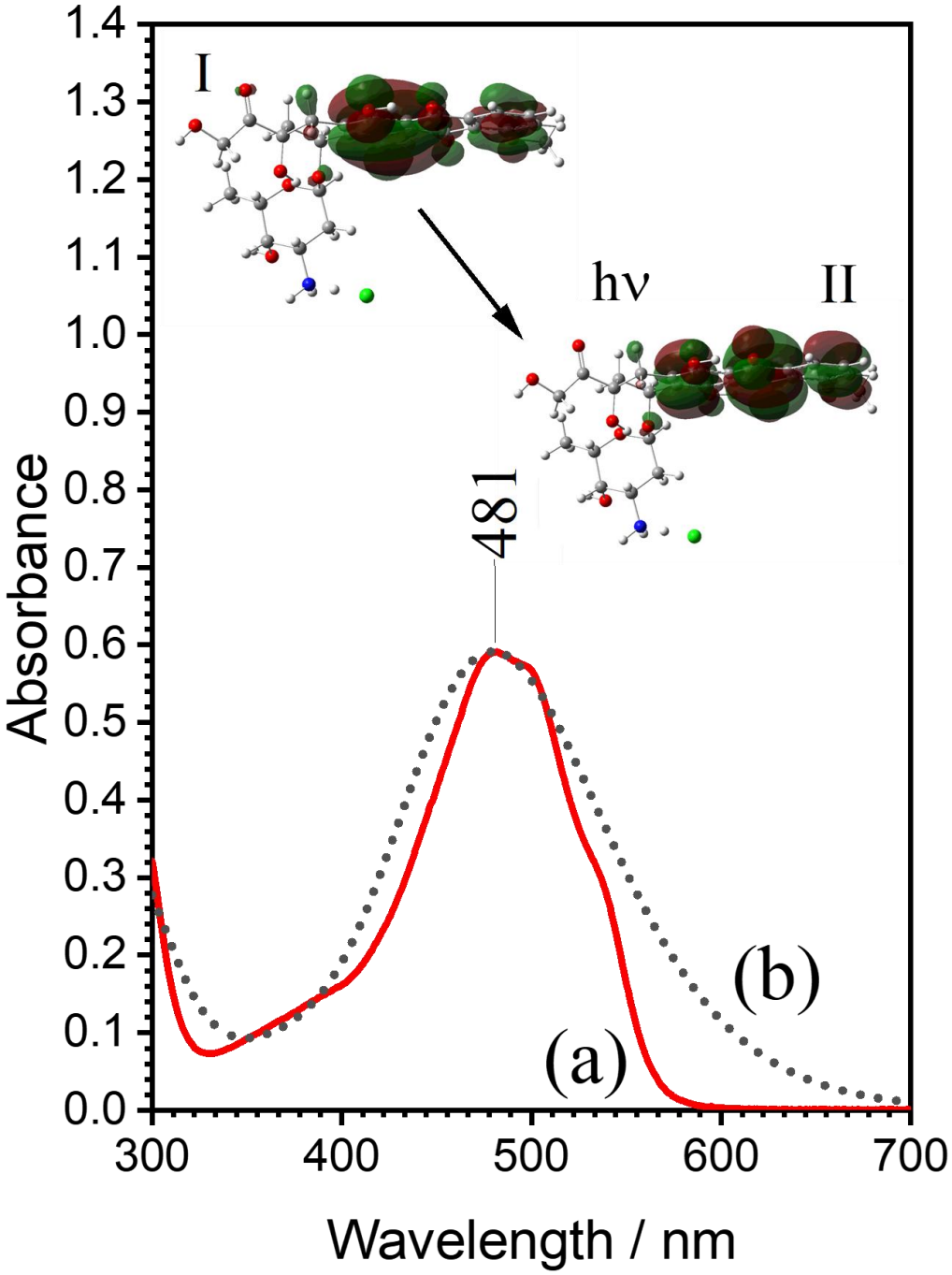

Figure S3. UV-Vis absorption spectra of (a) 1×10^{-3} mol L^{-1} doxorubicin aqueous solution, and (b) simulated with TD-DFT methodology B3LYP/6+31G(d,p), only singlet states. Inset: Natural Transition Orbitals of (I) fundamental state and (II) excited state.

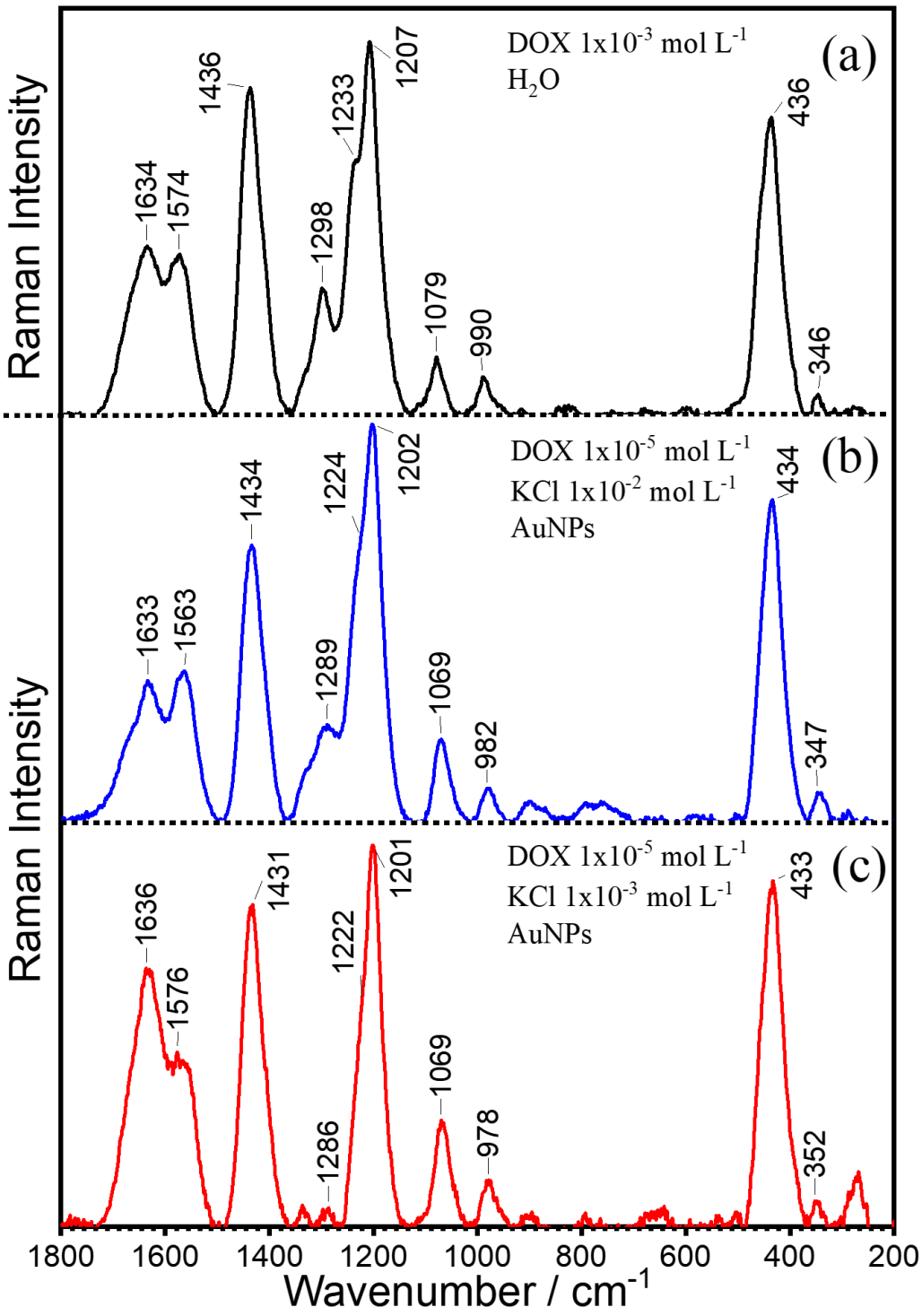

Figure S4. Raman spectrum of (a) 1×10^{-3} mol L^{-1} aqueous solution; SERS spectra of 1×10^{-5} mol L^{-1} doxorubicin adsorbed on AuNPs dispersion, modified with KCl with final concentration of (a) 1×10^{-2} mol L^{-1} and (b) 1×10^{-3} mol L^{-1}, obtained with λ_{ex} = 632.8 nm.

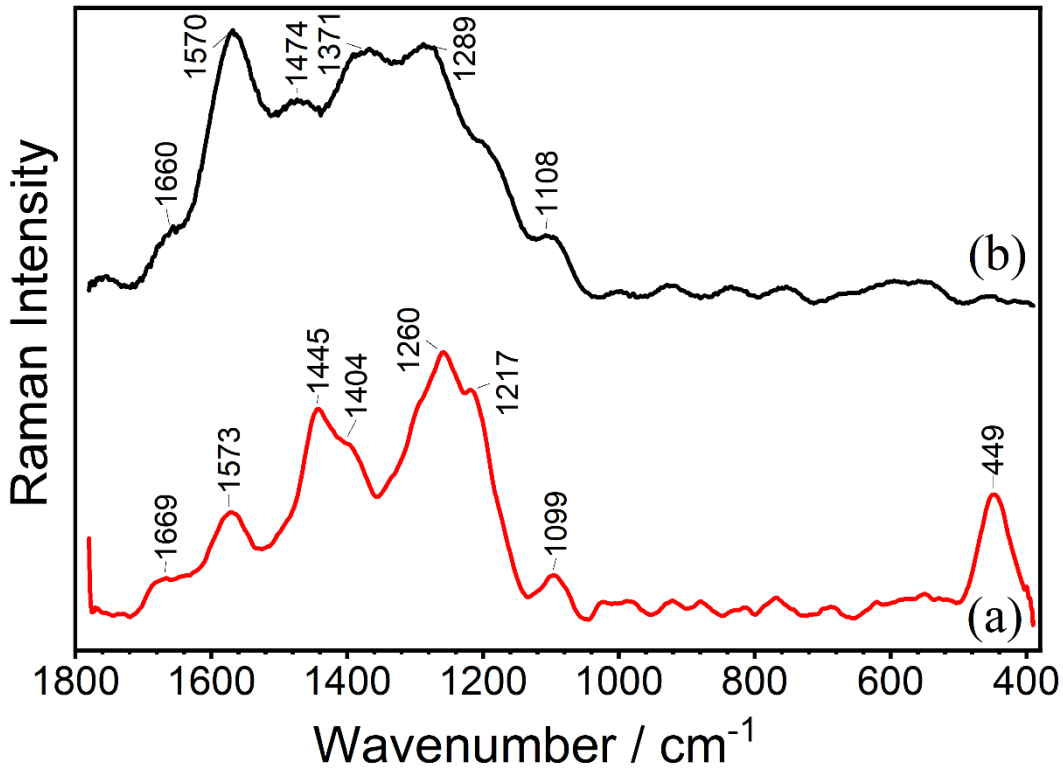

Figure S5. (a) Averaged 100 points, baseline corrected and smoothed SERS spectra of 1×10^{-4} mol L^{-1} doxorubicin adsorbed on AuNPs dry film, modified before drying with KCl, with final concentration of 1×10^{-3} mol L^{-1}; (b) averaged 62 points SERS spectra of 1×10^{-5} mol L^{-1} doxorubicin adsorbed on AuNPs dry film, modified before drying with β-ME, with final concentration of 1×10^{-8} mol L^{-1}. Spectra obtained with λ_{ex} = 632.8 nm.

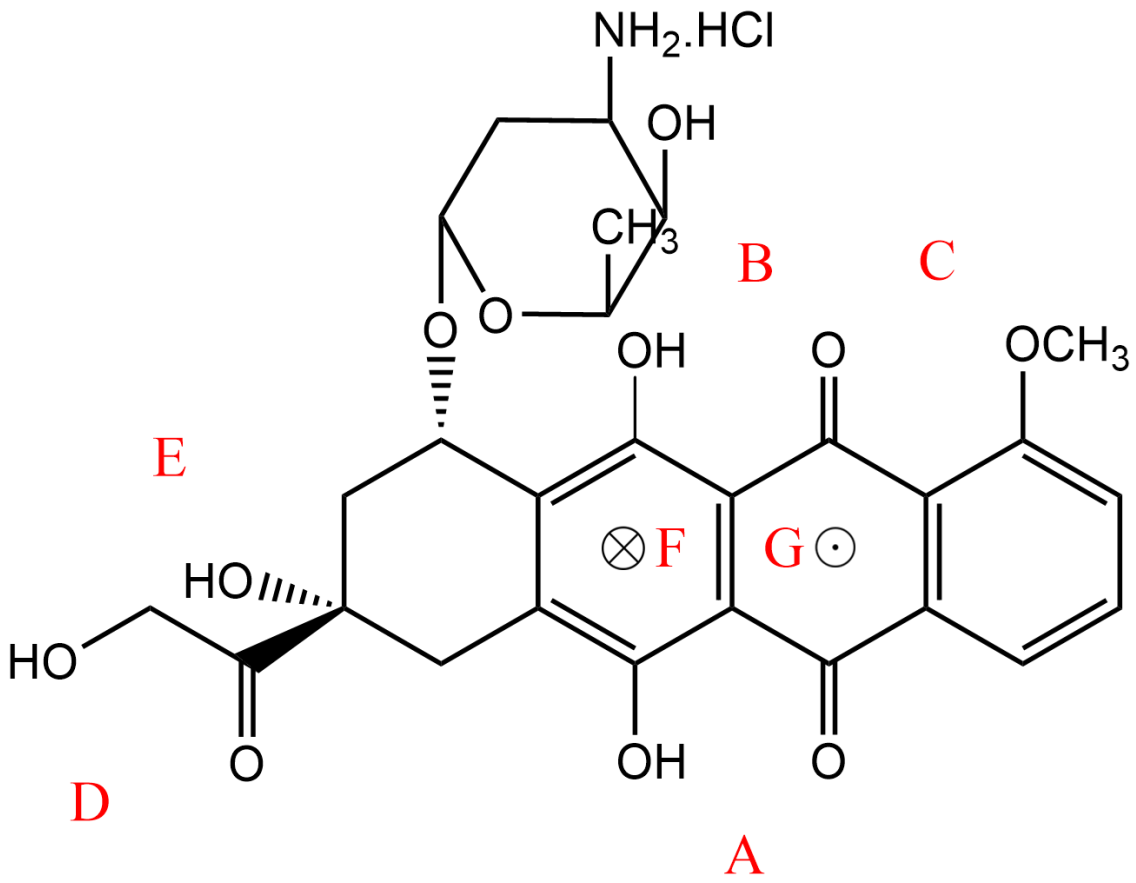

Figure S6. Positions where Au_2 dimer adsorption were tested. The ⊗ symbol indicates a position in a colinear plane below the anthraquinones plane, and Θ symbol indicates a position in a colinear plane above the anthraquinones plane.

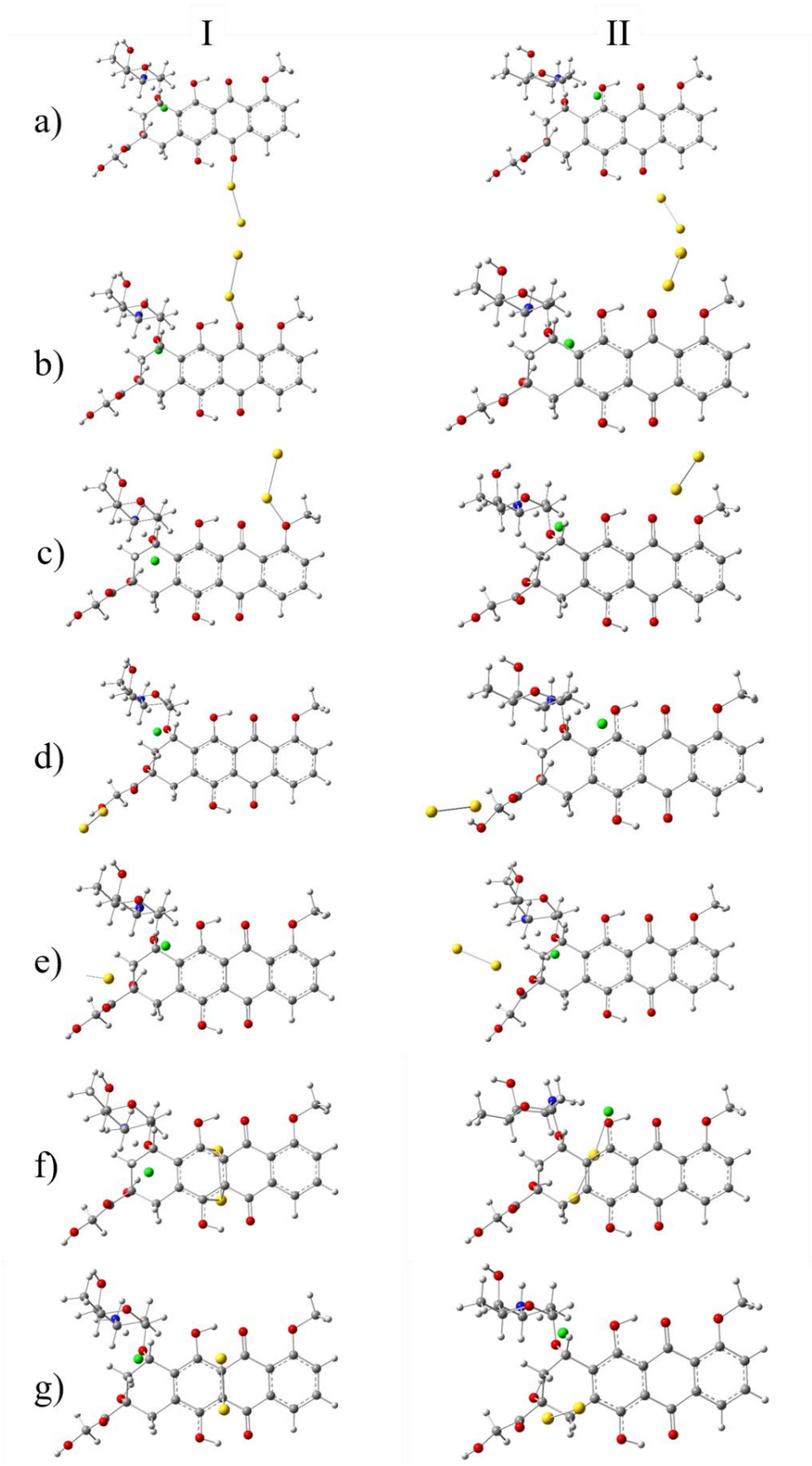

Figure S7. Positions, from 'a' to 'g', with initial position of Au_2 dimer (I) and the resulting converged geometry (II).

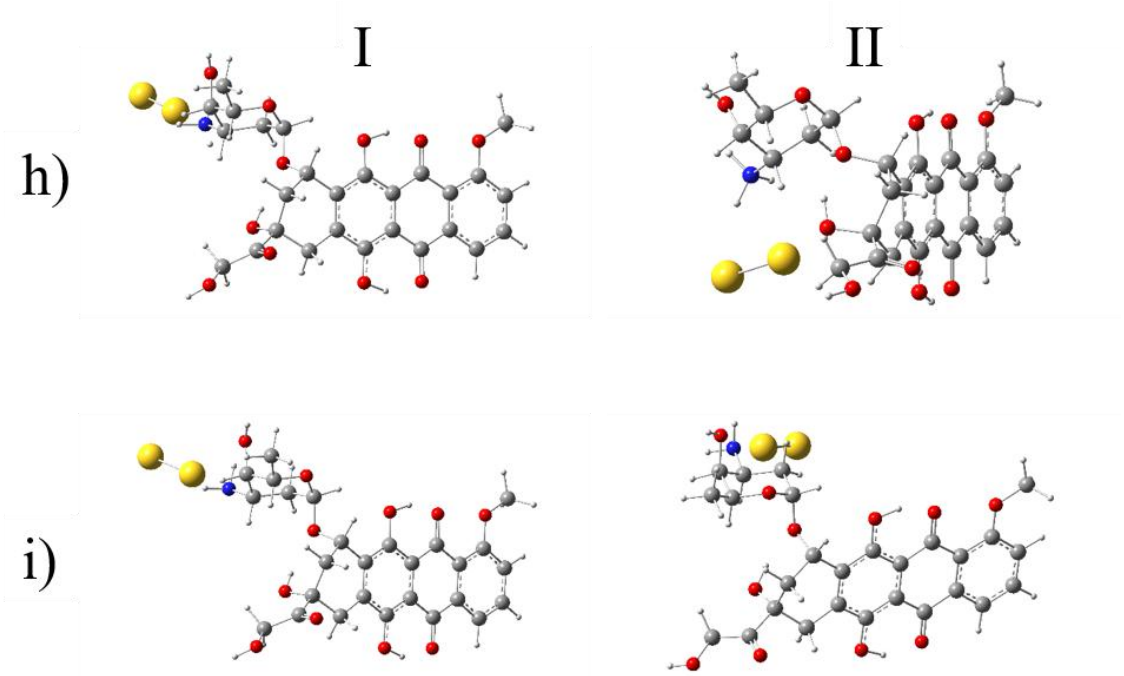

Figure S8. Positions, from 'h' and 'i', where Au_2 dimer adsorption were tested (I), and the resulting geometry (II). (h) Adsorption were tested for protonated DOX hydrochloride by suppressing the chlorine anion, and (i) for neutral DOX, suppressing the chloridric acid.

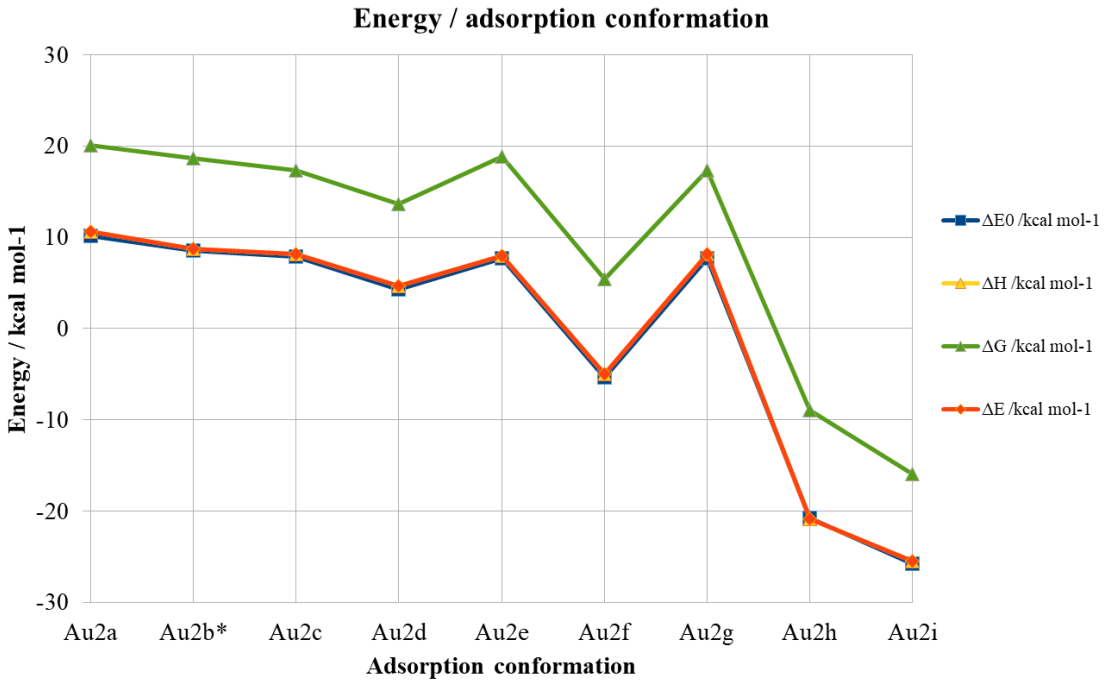

Figure S9. DOXH-Cl-Au_2 (Au_2a to Au_2g), DOXH-Au_2 (Au_2h) and DOX-Au_2 (Au_2i) dimer conformation interaction energies. (ΔE_0: sum of electronic and zero-point energies; ΔE: thermically corrected electronic energy; ΔH: sum of electronic and thermal enthalpies; ΔG: sum of electronic and thermal free energies).

Table S1. DOX-Au_2 dimer interaction sites and energies involved

Site	ΔE_0 / (kcal mol^{-1})	ΔE / (kcal mol^{-1})	ΔH / (kcal mol^{-1})	ΔG / (kcal mol^{-1})
Au2a	10.18	11.26	10.67	20.12
Au2b[a]	8.53	9.33	8.74	18.69
Au2c	7.84	8.79	8.20	17.38
Au2d	4.32	5.29	4.70	13.66
Au2e	7.74	8.60	8.00	18.81
Au2f	–5.36	–4.36	–4.96	5.40
Au2g	7.68	8.72	8.13	17.34
Au2h[b]	–20.77	–20.21	–20.81	–8.90
Au2i[c]	–25.72	–24.90	–25.49	–15.91

[a]Saddle point; [b]protonated DOX by suppressing Cl^-; [c]neutral DOX.

The lowest energy value, from Neutral DOX, do not represent the adsorption conditions used in this work, since such a species is present only in basic pH. The second lower energy structure is also improbable to be present in the gold surface, since the DOX solution was prepared from hydrochloride species that, when dissolved, presents chloride ions that have high affinity by the metallic surface.

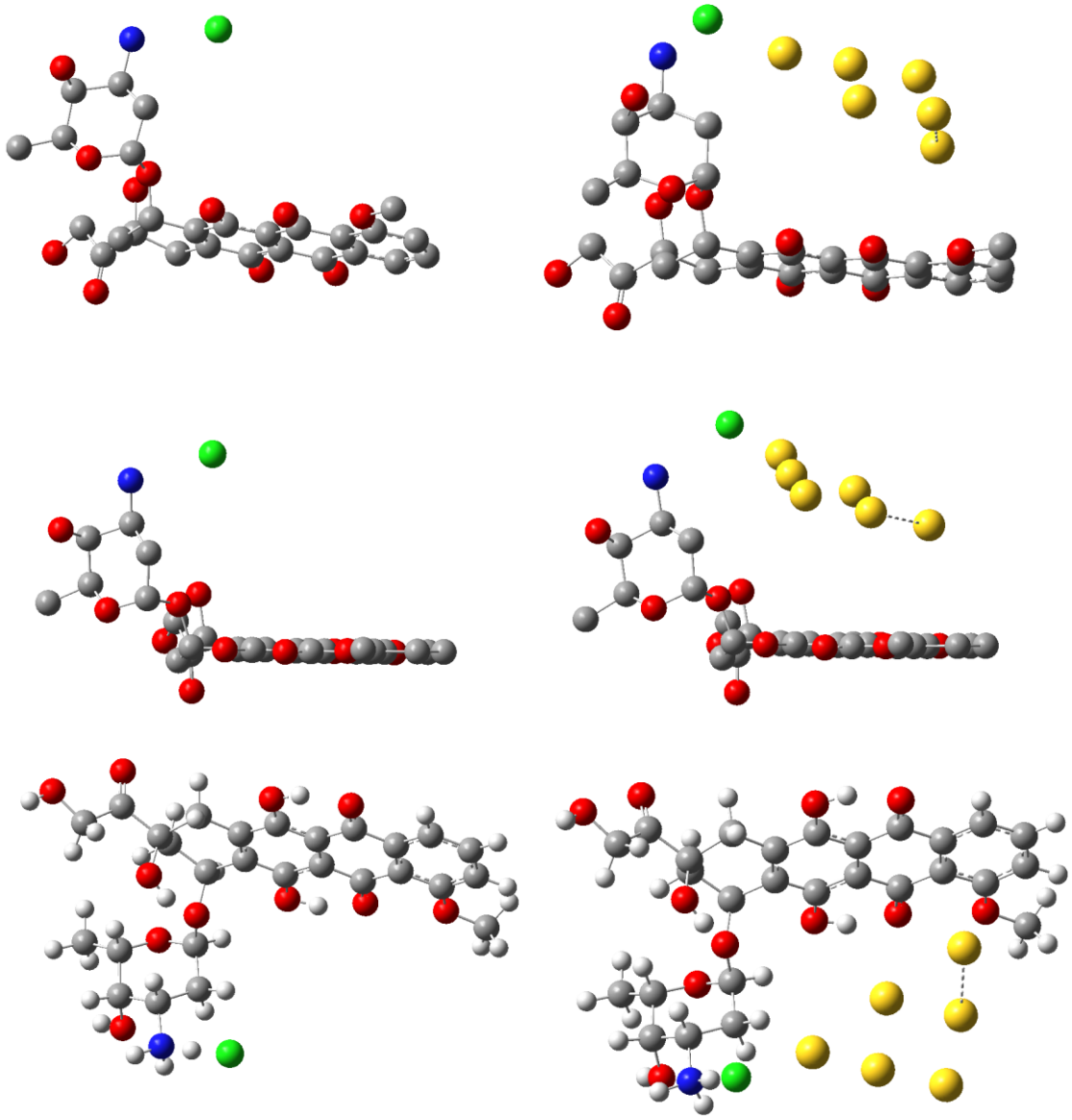

Figure S10. Different views from optimized geometries of DOX and DOX-Au_6.

Table S2. Comparative SERS features of DOX results from literature

SERS[a] (KCl_{aq}) 632.8 nm	SERS[a] (KCl_{aq}) 1064 nm	SERS[a] (ME_{aq}) 1064 nm	SERS[b] AuNP 785 nm	SERS[c] AgNP 633 nm pH 7.4	SERRS[d] AgNP 514 nm	SERS[d] AgNP 1064 nm
1660	1685	1673		–	–	–
1637	1641	1654		1638(sh)	1642	1642
–	1618	1607		–	1607	–
1577	1583	1575		1586(sh)	1580	1579
–	1452	1466	1499	1456	1462	–
1432	–	–		1434	1436	1445
1410	1419	1416		1413	–	1411
1287	–	1299	1299	1296	–	1276
–	1284	1283		–	–	–
1234	–	–	1235	1224	1255	1248
1202	1138	–	1208	1210	1224	1214
1070	1080	1084		1082	–	1085
979	–	1014		990	–	937
–	–	826		–	–	–
–	796	799		795	–	–
–	507	494		504	–	–
433	465	455	439	443	–	–

[a]This work; [b]Panikar *et al.*;[1] [c]Gautier *et al.*;[2] [d]Beljebbar *et al.*[3]

Table S3. Cartesian coordinates for DOX optimized geometry

Atom	x	y	z	Atom	x	y	z
O	5.807904	−2.200638	−1.202417	C	−3.315731	3.685354	−0.139128
O	3.307265	−1.564545	−1.532645	C	−4.458737	3.749180	0.860175
O	0.876464	−1.025618	−1.784436	H	−5.036939	2.817071	0.772812
H	1.766305	−1.489974	−1.866837	H	−4.019756	3.743709	1.869301
O	−1.865588	−0.507512	−0.450521	C	5.016360	0.927421	0.524794
O	−2.810677	1.665145	1.054638	C	4.841725	−0.244044	−0.256118
H	−2.465830	0.766860	0.923857	C	2.570729	1.528112	0.254976
O	1.608854	3.501956	1.232815	C	2.391123	0.353562	−0.528870
H	2.565908	3.552338	1.510683	C	0.188465	2.075726	−0.005026
O	4.065825	2.883745	1.477890	C	0.016141	0.931497	−0.769217
O	−3.151663	4.521208	−1.004011	C	6.908277	−3.084121	−1.406568
O	−5.239706	4.898668	0.609244	H	7.281631	−3.482657	−0.455911
H	−5.909446	4.970395	1.300245	H	7.722653	−2.589768	−1.949437
O	−5.032109	−3.816132	−0.524656	H	6.510862	−3.899266	−2.011227
H	−5.752837	−3.778373	−1.165697	C	−2.226506	−1.723014	−1.090920
O	−3.445935	−1.600287	−1.810358	H	−1.479270	−1.963192	−1.850586
N	−3.602671	−3.790494	1.820088	C	−2.291849	−2.820099	−0.029426
H	−2.584056	−3.856069	2.523852	H	−2.355951	−3.780187	−0.552074
H	−3.740761	−4.662135	1.305592	H	−1.378025	−2.813146	0.569389
H	−4.392400	−3.686179	2.458509	C	−3.518990	−2.648827	0.871025
C	6.257002	1.259546	1.075068	H	−3.405141	−1.748942	1.483410
H	6.339475	2.164508	1.664802	C	−4.797823	−2.522890	0.031741
C	7.348867	0.425112	0.858195	H	−5.641441	−2.238747	0.683401
H	8.317199	0.673174	1.282529	C	−4.618790	−1.403528	−1.012623
C	7.213237	−0.735054	0.099371	H	−4.519967	−0.467091	−0.442800
H	8.076226	−1.370081	−0.053962	C	−5.790192	−1.274491	−1.978352
C	5.973621	−1.085160	−0.463912	H	−5.637552	−0.416473	−2.637836
C	3.506993	−0.555643	−0.820352	H	−6.729489	−1.127023	−1.434558
C	1.113694	0.063309	−1.035396	H	−5.876868	−2.160049	−2.617513
C	−1.344617	0.547398	−1.313367	Cl	−1.277043	−3.857193	3.457401
H	−1.231977	0.136518	−2.320746				
C	−2.318104	1.725736	−1.351156				
H	−3.316983	1.357539	−1.603185				
H	−2.014900	2.422047	−2.140070				
C	−2.341564	2.493636	−0.016292				
C	−0.932650	3.045355	0.285075				
H	−0.772350	3.954010	−0.309482				
H	−0.886402	3.351885	1.334547				
C	1.482306	2.380387	0.509043				
C	3.882251	1.851722	0.795298				

Table S4. Cartesian coordinates for DOX-Au_6 optimized geometry

Atom	x	y	z	Atom	x	y	z
O	−3.044491	3.053516	3.172037	C	0.039614	4.790849	−0.227730
O	−0.558500	2.304455	3.068075	C	7.231448	2.778569	−0.439576
O	1.782547	1.470272	2.914936	C	7.984965	2.131238	−1.589971
H	0.828582	1.610391	3.218499	H	8.095745	1.060793	−1.361174
O	4.148575	0.083646	1.213386	H	7.344287	2.188519	−2.483465
O	5.643457	1.052334	−0.922630	C	−1.291593	4.726936	0.431841
H	4.920509	0.529399	−0.542387	C	−1.520379	3.880940	1.547059
O	2.644229	4.790314	−1.374054	C	1.114393	3.947412	0.277969
H	1.797492	5.278198	−1.575907	C	0.887431	3.094815	1.392271
O	0.222874	5.556381	−1.199480	C	3.442039	3.171060	0.151109
O	7.688838	3.694463	0.213103	C	3.215689	2.326520	1.230164
O	9.226071	2.781289	−1.764667	C	−4.351786	2.955086	3.732224
H	9.661970	2.405095	−2.538900	H	−5.075261	2.594063	2.992182
O	4.943913	−4.212574	2.529873	H	−4.683651	3.916057	4.143855
H	5.396283	−4.309210	3.377382	H	−4.262234	2.226429	4.538044
O	4.642736	−1.259650	3.080051	C	3.670135	−0.913254	2.100114
N	4.082933	−4.097135	−0.004913	H	2.825440	−0.530647	2.674034
H	3.529104	−3.911942	−0.918114	C	3.261399	−2.126455	1.261683
H	3.529325	−4.674624	0.633363	H	2.730446	−2.816802	1.925327
H	4.899817	−4.649667	−0.277408	H	2.572604	−1.815349	0.470274
C	−2.307629	5.527403	−0.097374	C	4.494573	−2.821453	0.680663
H	−2.084152	6.157862	−0.949728	H	4.961976	−2.202456	−0.090116
C	−3.576111	5.493095	0.475393	C	5.518879	−3.148253	1.773326
H	−4.373708	6.108915	0.070162	H	6.460838	−3.489200	1.310635
C	−3.837542	4.669558	1.567702	C	5.831648	−1.872000	2.579973
H	−4.833001	4.654851	1.992837	H	6.332999	−1.185916	1.880985
C	−2.827067	3.858983	2.115852	C	6.745968	−2.117222	3.774080
C	−0.416727	3.044438	2.069567	H	6.989579	−1.165798	4.253036
C	1.938628	2.289268	1.860193	H	7.680349	−2.594495	3.460019
C	4.318549	1.430583	1.763586	H	6.258487	−2.740494	4.532594
H	4.243738	1.361130	2.851674	Cl	2.802994	−3.649173	−2.652869
C	5.710068	1.929564	1.374902	Au	0.805854	−2.341126	−1.810304
H	6.456839	1.183688	1.665302	Au	−1.193929	−2.332284	0.045093
H	5.933495	2.849177	1.925316	Au	−0.895885	−0.227630	−1.747701
C	5.819446	2.232974	−0.130958	Au	−3.257293	−2.236795	1.842714
C	4.790667	3.318285	−0.515121	Au	−2.728119	1.811269	−1.661313
H	5.194377	4.304495	−0.250807	Au	−3.142629	−0.128907	0.159388
H	4.664157	3.320240	−1.602268				
C	2.379670	3.987721	−0.332167				

References

1. Panikar, S. S.; Banu, N.; Escobar, E. R.; García, G. R.; Cervantes-Martínez, J.; Villegas, T. C.; Salas, P.; De la Rosa, E.; *Talanta* **2020**, *218*, 121138. [Crossref]

2. Gautier, J.; Munnier, E.; Douziech-Eyrolles, L.; Paillard, A.; Dubois, P.; Chourpa, I.; *Analyst* **2013**, *138*, 7354. [Crossref]

3. Beljebbar, A.; Sockalingum, G. D.; Angiboust, J. F.; Manfait, M.; *Spectrochim. Acta, Part A* **1995**, *51*, 2083. [Crossref]